Ionospheric effects of whistler waves from rocket-triggered lightning

B. R. T. Cotts,[1] M. Gołkowski,[1] and R. C. Moore[2]

Received 15 October 2011; revised 13 November 2011; accepted 15 November 2011; published 24 December 2011.

[1] Lightning-induced electron precipitation (LEP) is one of the primary mechanisms for energetic electron loss from Earth's radiation belts. While previous works have emphasized lightning location and the return stroke peak current in quantifying lightning's role in radiation belt electron loss, the spectrum of the lightning return stroke has received far less attention. Rocket-triggered lightning experiments performed at the International Center for Lightning Research and Testing (ICLRT) at Camp Blanding, Florida, provide a means to directly measure the spectral content of individual lightning return strokes. Using an integrated set of numerical models and directly observed rocket-triggered lightning channel-base currents we calculate the latitudinal dependence of the precipitation signature. Model results indicate that rocket-triggered lightning may produce detectable LEP events and that return strokes with higher ELF (3 Hz–3 kHz) content cause proportionally more ionospheric ionization and precipitate more electrons at higher latitudes than return strokes with proportionally higher VLF (3 kHz–30 kHz) content. The predicted spatio-temporal signature of the induced electron precipitation is highly dependent upon the return stroke spectral content. As a result, we postulate that rocket-triggered lightning experiments enable us to the estimate the spectral profile of energetic electrons precipitated from the Earth's radiation belts. **Citation:** Cotts, B. R. T., M. Gołkowski, and R. C. Moore (2011), Ionospheric effects of whistler waves from rocket-triggered lightning, *Geophys. Res. Lett.*, *38*, L24805, doi:10.1029/2011GL049869.

1. Introduction

[2] One of the dominant natural loss mechanisms for energetic radiation belt electrons in the range $2 < L < 3$ is the electron interaction with lightning-generated whistler mode waves [*Abel and Thorne*, 1998]. Understanding the removal of these electrons has received significant attention in the past [e.g., *Thomson and Dowden*, 1977; *Yip et al.*, 1991; *Johnson et al.*, 1999; *Clilverd et al.*, 2002; *Peter and Inan*, 2007] due to the fact that the on-board electronics of spacecraft are damaged by these high energy fluxes and are particularly vulnerable during periods of enhanced geomagnetic activity [*Baker et al.*, 2004]. In addition, the deposition of energy within the ionosphere by electrons that are precipitated (i.e., removed) from the radiation belts can significantly affect the propagation of subionospheric VLF transmitter signals, potentially reducing the amount of received power by >3 dB for several minutes or more [e.g., *Inan et al.*, 1988; *Sampath et al.*, 2000; *Peter et al.*, 2006]. These VLF scattering observations are commonly referred to as lightning-induced electron precipitation (LEP) events.

[3] Much of the previous work has investigated the effects of lightning peak current on electron precipitation. *Lauben et al.* [2001] showed that the magnitude of pitch angle scattering (and hence the number of precipitating electrons) is linearly related to the magnitude of the lightning-launched electric field. *Peter and Inan* [2007] demonstrated that it is possible to estimate the number and total energy of precipitating electrons from an observed change in the received amplitude of subionospherically propagating VLF transmitter signals passing through the precipitation region. While it is widely accepted that the frequency content of the lightning source can have a significant effect on the characteristics of LEP events, few studies have focused on quantifying these effects. All previous investigations that address the source lightning spectrum assume a theoretical form for the source lightning frequency content, and none have considered the effects of varying the source frequency content. Moreover, previous works have relied on simple local loss cone calculations and have not included the effect of atmospheric backscatter as described by *Cotts et al.* [2011]. For example, *Chang and Inan* [1985] investigated the precipitation at a single location due to an assumed Gaussian-shaped lightning spectrum with a peak at 5 kHz, while *Inan et al.* [1988] investigated the *L*-dependence of precipitation for a whistler-mode wave with constant intensity between 0.2 kHz and 6 kHz. *Rodger et al.* [2003] investigated the difference in LEP event recovery for two different assumed electron precipitation spectra (affected both by geomagnetic conditions and source lightning frequency content). While *Albert* [2001] investigated the diffusion coefficient of electrons of various pitch angles and as a function of whistler frequency (a key component in the LEP process), there has been no systematic analysis on the role of lightning spectral content on the characteristics of LEP events.

[4] The difficulty in calculating the dependence of LEP on source lightning frequency content lies in accurately determining the latter. We address this problem by investigating the geographic precipitation pattern for rocket-triggered lightning flashes at the International Center for Lightning Research and Testing (ICLRT) at Camp Blanding, Florida where the lightning channel-base current is directly measured. Wave particle interaction simulations driven by these rocket-triggered lightning measurements provide a unique opportunity for investigating the potential effects of source lightning spectrum on radiation belt electron loss. Using directly-measured lightning return stroke currents we demonstrate for the first time that the variety of spectra radiated by rocket-

[1]Department of Electrical Engineering, University of Colorado Denver, Denver, Colorado, USA.
[2]Department of Electrical and Computer Engineering, University of Florida, Gainesville, Florida, USA.

0094-8276/11/2011GL049869

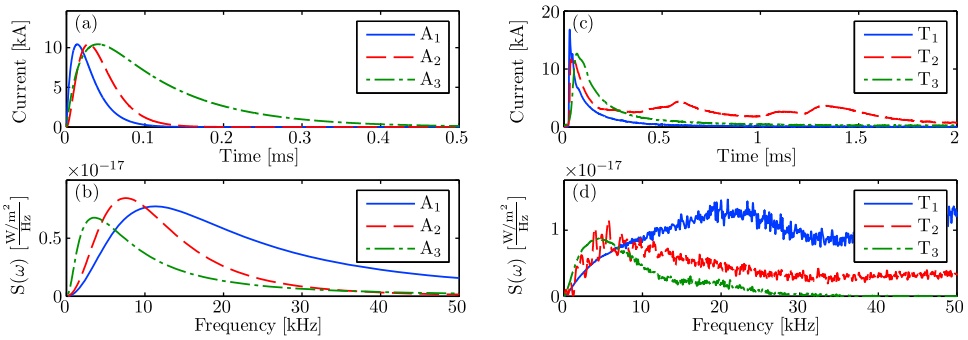

Figure 1. (a–d) Time domain current waveforms and power spectral density for analytical lightning models and rocket-triggered lightning return strokes.

triggered lightning produce a measurable difference in the signature of LEP events. To facilitate comparison with past work, Section 2 discusses analytical estimates of the source lightning content while Section 3 discusses the effects of specific observations of rocket-triggered lightning-flashes.

2. Theoretical Source Lightning Spectrum

[5] An analytical waveform which has received widespread use in past work is that of a double-exponential [*Bruce and Golde*, 1941], given in equation (1) with several examples shown in Figure 1a. This simple analytical form reflects the characteristics of a typical lightning return stroke reasonably well and allows straight-forward spectral analysis. A more realistic model was later introduced, containing an extra rise-time term [*Dennis and Pierce*, 1964] as shown in equation (2). Model results characterizing the LEP events produced by these two analytical waveforms will be compared with those produced by rocket-triggered lightning.

$$I_1(t) = I_0\left(e^{-at} - e^{-bt}\right) \tag{1}$$

$$I_2(t) = I_0\frac{\nu_0}{\gamma}\left(e^{-at} - e^{-bt}\right)\left[1 - e^{-\gamma t}\right] \tag{2}$$

[6] In the above equations, I_0 is a model scaling factor for the peak current, and a, b, γ, and ν_0 are model parameters controlling the rise- and decay-time of the current waveform. Note that as in past work I_0 is defined in Amperes in equation (1) and in kilo-Amperes in equation (2). The electric field due to a vertical lightning return stroke observed at location (R,ξ) is given by *Uman* [1984, p. 127] as:

$$E = \mu_0\frac{h_e\sin\xi}{2\pi R}\left[\frac{dI}{dt}\right], \tag{3}$$

where R is the distance from the source to the observation point (determined as by *Lauben et al.* [2001]), ξ is angle of the wave with respect to local zenith and h_e is the height of the initial charge (assumed to be 5 km). Substituting equations (1) or (2) into equation (3) yields the far-field power spectral density (PSD), $S(\omega)$:

$$S_1(\omega) = K_0\frac{\omega^2(a-b)^2}{(\omega^2+a^2)(\omega^2+b^2)} \tag{4}$$

$$S_2(\omega) = K_0\left(\frac{\nu_0}{\gamma}\right)^2\frac{\left(\delta^2+4\omega^2\right)(a\gamma\omega - b\gamma\omega)^2}{(a^2+\omega^2)(b^2+\omega^2)(\alpha^2+\omega^2)\left(\beta^2+\omega^2\right)} \tag{5}$$

where K_0 includes all physical constants:

$$K_0 = \frac{1}{Z_0}\left(\frac{\mu_0 h_e I_0}{2\pi}\right)^2\left(\frac{\sin\xi}{R}\right)^2, \text{ and}$$

$$\alpha = a+\gamma, \quad \beta = b+\gamma, \quad \delta = a+b+\gamma.$$

$S(\omega)$ is in units of W−m^{-2} Hz^{-1}, ω is the radial frequency in rad/sec, and Z_0 and μ_0 are the intrinsic impedance (∼377 Ω) and permeability ($4\pi \times 10^{-7}$ H/m) of free space, respectively.

[7] We first vary the parameters of the analytical source lightning spectrum and illustrate the effect on LEP production. Varying the model parameters as shown in Table 1, yields the three waveforms shown in Figure 1a. Each waveform has been chosen to reflect the same peak current (∼10 kA) as a typical rocket-triggered return stroke [*Nag et al.*, 2011], but with a peak in the PSD at varying frequencies as shown in Figure 1b. Waveform A_1 represents a typical lightning flash with a peak in the PSD at ∼10 kHz [*Uman*, 2001, p. 118], while Waveforms A_2 and A_3 exhibit PSD maxima at frequencies of ∼7.5 kHz and ∼3.5 kHz, respectively.

[8] Following the methodology of *Bortnik et al.* [2006], we use the Whistler-Induced Particle Precipitation (WIPP) code to calculate the magnitude of electron pitch angle scattering at each L-shell as a function of time and electron energy for each of the waveforms in Figure 1a. The lightning location for each of these simulations is the ICLRT with geographic coordinates of 30°N, 278°E (40°N, 350°E geomagnetic). Using the calculated pitch angle change over the first two seconds of precipitation we then calculate the altitude profile of the ionospheric deposition. *Cotts et al.* [2011] demonstrated that precipitating electrons backscatter from the atmosphere and are subsequently incident on the conjugate atmosphere. This process can repeat many times, creating ionization with each atmospheric interaction, but the first two depositions are dominant at this longtitude. Figure 2a shows an example of secondary ionization for the first two deposition profiles (dashed lines) in the Northern Hemisphere

Table 1. Lightning Model Parameters as Described in the Text

Waveform	I_0 (kA)	a	b	γ	ν_0 (m/s)
A_1	41.7	5×10^4	1×10^5	—	—
A_2	41.7	5×10^4	1×10^5	3×10^3	5.0×10^7
A_3	19.5	1×10^4	5×10^4	—	—

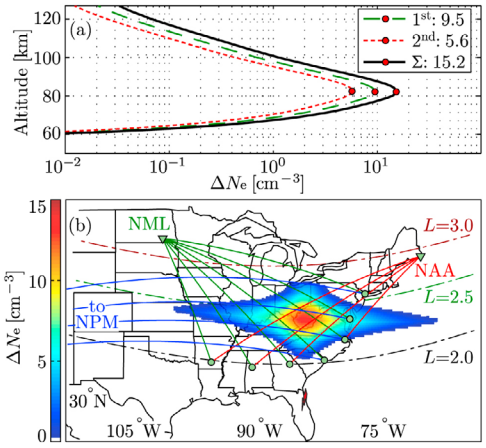

Figure 2. (a) Ionospheric electron density enhancement as a function altitude. (b) Example disturbance for waveform T_3 with VLF remote-sensing propagation paths.

as well as the sum total of the two curves shown in the solid line.

[9] In order to track the electron resonance dynamics at $L < 2$ we include electrons energies up to 1 MeV. The peak deposition magnitude in the solid black curve in Figure 2a is a quantitative measure representing the precipitation signature at a particular location. This calculation is repeated for each of the analytical waveforms $A_1 - A_3$ with results shown in Figure 3a. The results show that not only does the lightning spectral content influence the LEP signature, but it also significantly determines which regions of the magnetosphere are primarily affected. The lightning return strokes with relatively higher ELF frequency content create a peak in precipitated flux at higher *L*-shells. *Bortnik et al.* [2006] showed that lightning location is the dominant factor in determining the *L*-dependence of the precipitation signature. The results in Figures 1 and 3, however, demonstrate that for a specified location the causative lightning PSD has a significant and measurable effect on the LEP precipitation signature.

3. Rocket Triggered Lightning Spectrum

[10] The analytical description described in Section 2 is a reasonable approximation to the current of a typical lightning return stroke. However, actual lightning return strokes are often far more complex. For example, sprite-producing lightning often contains a large continuing current, which may persist for 10's of milliseconds [e.g., *Cummer and Füllekrug*, 2001; *Li et al.*, 2008] and is not well-modeled by a simple analytical expression. On the other hand, direct measurements of the lightning channel-base current during rocket-triggered lightning flashes can provide full knowledge of the current waveform. The observations reported here were obtained during rocket-and-wire-triggered lightning experiments on 29 March 2009 at the ICLRT. Detailed reports regarding lightning experiments at the ICLRT may be found in numerous publications [e.g., *Jerauld et al.*, 2008; *Nag et al.*, 2011]. The lightning channel-base current measurements presented in this work were performed using a 1.0-mΩ coaxial shunt resistor with upper cutoff frequency of 8 MHz at the base of the rocket trailing wire.

[11] Three return strokes from a single rocket triggered flash on 29 March 2009 are shown in Figure 1c. While each stroke is qualitatively similar to those shown in Figure 1a, they contain significantly more structure than can be represented by an analytic approximation. This fact is more apparent from the PSD shown in Figure 1d. Triggered stroke T_1 is the largest of the three and has a peak current of ~17 kA and a broad spectral peak near 20 kHz. Stroke T_3 has a peak current of ~13 kA and a narrower spectral peak near 4.3 kHz. The continuing currents of stroke T_2 (peak current of ~12 kA) produce several narrow spectral peaks, the three largest of which are near 4.0 kHz, 5.5 kHz and 7 kHz, on top of a PSD which decays with frequency more gradually than T_3. Calculating the deposition as a function of *L*-shell for the rocket-triggered lightning waveforms yields results similar to those presented in Section 2. As shown in Figure 3b, the peak change in electron density is ~15 elec/cm^3, which is only slightly higher than for the analytical (10 kA) waveforms shown in Figure 3a. As shown by *Cotts et al.* [2011, Figure 9], such electron density changes can produce VLF amplitude changes on the order of 0.2 dB, a change that is detectable in practice, as discussed below.

[12] Figure 3b demonstrates that the lightning PSD significantly alters the regions of the ionosphere and magnetosphere which are most affected by a particular lightning return stroke. For the investigated return strokes, the stroke with the largest ELF content creates a peak in precipitated flux at higher *L*-shells than a "typical" lightning stroke (e.g., T_1). As shown by Figure 3b, the peak in the precipitation region for waveform T_3 is shifted more than 300 km poleward (0.3 *L*) from that of T_1. In addition, the total precipitation (summed over all *L*-shells) for all return strokes are within ~10% of each other, despite the fact that waveform T_1 has a peak current ≥30% larger than that of either T_2 or T_3. This indicates that return strokes with stronger ELF components are more efficient at precipitating energetic electrons from the radiation belts. The shift to higher *L*-shell is due to a combination of lower frequency whistler waves propagating to higher *L*-shells [e.g., *Bortnik et al.*, 2003] and to a decreasing electron cyclotron frequency with increasing *L*. While the former primarily shifts the precipitation region poleward, the latter shifts the resonant energy of electrons to lower energies (where there are a larger number of particles) resulting in a higher total precipitated energy flux. For

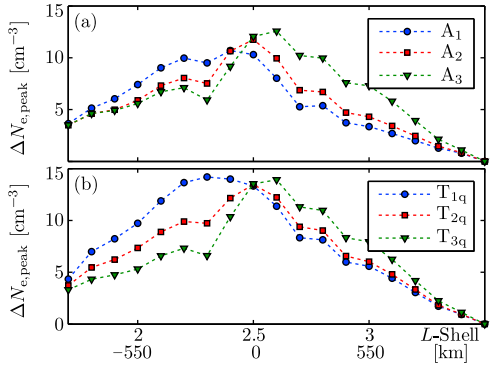

Figure 3. Peak ionospheric electron density enhancement as a function of *L*-shell for (a) analytical lightning waveforms and (b) triggered lightning waveforms.

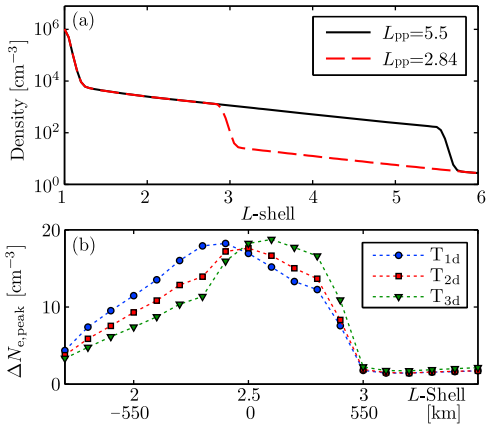

Figure 4. (a) Magnetospheric electron density profiles used in simulations. (b) Peak precipitation vs. *L*-shell using a disturbed magnetosphere.

example, at L = 2.3 whistler waves of 0.5–4.5 kHz experience first order resonance with 0.1–1 MeV electrons while at L = 2.7 the resonant frequency range for these energies decreases to 0.2–2 kHz. The net result is that 0.1–1 MeV electrons are precipitated only by the ELF frequency components and hence lightning waveforms which have higher PSD at ELF frequencies produce proportionally more ionization.

[13] An array of VLF receivers along the eastern coast of the U.S. (e.g., as shown in Figure 2b) can capture this *L*-dependent precipitation signature in a manner very similar to previous work performed in Colorado [e.g., *Peter and Inan*, 2007]. Such an array, with receivers spaced every 0.1 *L* (∼110 km), would provide a metric by which future LEP events could be compared. Similarly, an array of VLF receivers (with longitudinal spacing) in the southeastern U.S. maybe used to simultaneously quantify the longitudinal extent of the precipitation region. In the absence of a measurement station at every 0.1 *L*, Figure 3b also indicates that it is sufficient to perform observations at only a few locations. The shift in the resultant peak deposition among different source waveforms is large enough (0.3 *L* or >300 km) that the ratio of the deposition at just two separate *L*-shells suffices to differentiate among the precipitation signatures considered here. As shown in Figure 3b the ratio of the peak deposition at L = 2.3 and the peak deposition at L = 2.7 for lightning waveforms T_1, T_2 and T_3 is 1.7, 1.0 and 0.6, respectively. The modal structure of a VLF transmitter signal passing through this precipitation region should vary little over this relatively small *L*-shell range (e.g., for the 21.4 kHz NPM transmitter in Lualualei, HI). Therefore the magnitude of an LEP event at these two *L*-shells should scale by the same ratio in VLF observations [*Peter and Inan*, 2007].

3.1. Variability of the Magnetosphere

[14] All simulations heretofore have used a magnetospheric cold electron density profile for quiet geomagnetic conditions (Plasmapause at L = 5.5). The specific magnetospheric profile (based upon work by *Tarcsai et al.* [1988]) is shown in Figure 4a along with a profile representing disturbed geomagnetic conditions (Plasmapause at L = 2.84, used by *Peter and Inan* [2007]). Because the cold magnetospheric electron density dominates the trajectory of lightning whistler waves it will also affect the *L*-dependence of LEP. To show the effect of disturbed geomagnetic conditions (disturbed conditions also influence the magnitude of observed LEP events [*Peter et al.*, 2006]) we model the same three triggered lightning strokes in Figure 1c using the disturbed profile represented by the dashed line of Figure 4a. The results are shown in Figure 4b where it is clear that the plasmapause at $L \simeq 3$ has a significant guiding-effect on the trajectory of the whistler waves resulting in very little precipitation outside this region. As a result of this guiding effect, the *L*-dependent precipitation signature tends to be slightly broader with a sharper drop-off when compared to the quiet conditions (Figure 3b). However, the *L*-dependence of the precipitation region seen in quiet geomagnetic conditions still holds. For this case the ratio of peak deposition at L = 2.3 and L = 2.7 for lightning waveforms T_1, T_2 and T_3 is 1.3, 0.9 and 0.6, respectively. Past observations of LEP events using VLF remote sensing [*Peter and Inan*, 2007] have demonstrated the ability to quantify LEP induced amplitude changes of less than 0.1 dB and experimental differentiation between observed ratios at least ten percent above or below unity is feasible using VLF remote sensing. The predicted ratios described in Figures 3b and 4b are therefore well within observable limits of VLF remote sensing experiments.

4. Conclusions

[15] The results described in Sections 2 and 3 indicate that differences in the causative lightning spectrum produce measurable differences in the *L*-dependent magnitude of LEP events. The precise lightning return stroke frequency content obtained from rocket-triggered measurements combined with a forward modeling numerical approach can provide an estimate not only of the total precipitated energy flux, but also a measure of the spectral profile of precipitating electrons. Rocket-triggered lightning thus allows for the controlled investigation of the LEP phenomena and greater understanding of the removal of energetic radiation belt electrons by lightning as well as quantification of the effect that precipitating electrons have on the subionospheric communication channel.

[16] **Acknowledgments.** This work is supported by DARPA grant HR0011-10-1-0061 to the University of Florida and by subcontract UF-EIES-1005017-UCD to University of Colorado Denver. Further support is provided by NSF grants AGS-0940248 and ANT-0944639 to the University of Florida.

[17] The Editor thanks two anonymous reviewers for their assistance in evaluating this paper.

References

Abel, B., and R. M. Thorne (1998), Electron scattering loss in Earth's inner magnetosphere 1. Dominant physical processes, *J. Geophys. Res.*, *103*, 2385–2396.

Albert, J. M. (2001), Comparison of pitch angle diffusion by turbulent and monochromatic whistler waves, *J. Geophys. Res.*, *106*, 8477–8482, doi:10.1029/2000JA000304.

Baker, D. N., S. G. Kanekal, X. Li, S. P. Monk, J. Goldstein, and J. L. Burch (2004), An extreme distortion of the Van Allen belt arising from the 'Hallowe'en' solar storm in 2003, *Nature*, *432*, 878–881, doi:10.1038/nature03116.

Bortnik, J., U. S. Inan, and T. F. Bell (2003), Frequency-time spectra of magnetospherically reflecting whistlers in the plasmasphere, *J. Geophys. Res.*, *108*(A1), 1030, doi:10.1029/2002JA009387.

Bortnik, J., U. S. Inan, and T. F. Bell (2006), Temporal signatures of radiation belt electron precipitation induced by lightning-generated MR

whistler waves: 1. Methodology, *J. Geophys. Res.*, *111*, A02204, doi:10.1029/2005JA011182.
Bruce, C. E. R., and R. H. Golde (1941), The lightning discharge, *J. Inst. Electr. Eng.*, *88*, 487–524.
Chang, H. C., and U. S. Inan (1985), Lightning-induced electron precipitation from the magnetosphere, *J. Geophys. Res.*, *90*, 1531–1541.
Clilverd, M. A., D. Nunn, S. J. Lev-Tov, U. S. Inan, R. L. Dowden, C. J. Rodger, and A. J. Smith (2002), Determining the size of lightning-induced electron precipitation patches, *J. Geophys. Res.*, *107*(A8), 1168, doi:10.1029/2001JA000301.
Cotts, B. R. T., U. S. Inan, and N. G. Lehtinen (2011), Longitudinal dependence of lightning-induced electron precipitation, *J. Geophys. Res.*, *116*, A10206, doi:10.1029/2011JA016581.
Cummer, S. A., and M. Füllekrug (2001), Unusually intense continuing current in lightning produces delayed mesospheric breakdown, *Geophys. Res. Lett.*, *28*, 495–498.
Dennis, A. S., and E. T. Pierce (1964), The return stroke of a lightning flash to earth as a source of VLF atmospherics, *Radio Sci.*, *68D*, 777–794.
Inan, U. S., W. C. Burgess, T. G. Wolf, D. C. Shater, and R. E. Orville (1988), Lightning-associated precipitation of MeV electrons from the inner radiation belt, *Geophys. Res. Lett.*, *15*, 172–175.
Jerauld, J., M. A. Uman, V. A. Rakov, K. J. Rambo, D. M. Jordan, and G. H. Schnetzer (2008), Electric and magnetic fields and field derivatives from lightning stepped leaders and first return strokes measured at distances from 100 to 1000 m, *J. Geophys. Res.*, *113*, D17111, doi:10.1029/2008JD010171.
Johnson, M. P., U. S. Inan, and D. S. Lauben (1999), Subionospheric VLF signatures of oblique (nonducted) whistler-induced precipitation, *Geophys. Res. Lett.*, *26*, 3569–3572, doi:10.1029/1999GL010706.
Lauben, D. S., U. S. Inan, and T. F. Bell (2001), Precipitation of radiation belt electrons induced by obliquely propagating lightning-generated whistlers, *J. Geophys. Res.*, *106*, 29,745–29,770, doi:10.1029/1999JA000155.
Li, J., S. A. Cummer, W. A. Lyons, and T. E. Nelson (2008), Coordinated analysis of delayed sprites with high-speed images and remote electromagnetic fields, *J. Geophys. Res.*, *113*, D20206, doi:10.1029/2008JD010008.
Nag, A., et al. (2011), Evaluation of U.S. National Lightning Detection Network performance characteristics using rocket-triggered lightning data acquired in 2004–2009, *J. Geophys. Res.*, *116*, D02123, doi:10.1029/2010JD014929.
Peter, W. B., and U. S. Inan (2007), A quantitative comparison of lightning-induced electron precipitation and VLF signal perturbations, *J. Geophys. Res.*, *112*, A12212, doi:10.1029/2006JA012165.
Peter, W. B., M. W. Chevalier, and U. S. Inan (2006), Perturbations of mid-latitude subionospheric VLF signals associated with lower ionospheric disturbances during major geomagnetic storms, *J. Geophys. Res.*, *111*, A03301, doi:10.1029/2005JA011346.
Rodger, C. J., M. A. Clilverd, and R. J. McCormick (2003), Significance of lightning-generated whistlers to inner radiation belt electron lifetimes, *J. Geophys. Res.*, *108*(A12), 1462, doi:10.1029/2003JA009906.
Sampath, H. T., U. S. Inan, and M. P. Johnson (2000), Recovery signatures and occurrence properties of lightning-associated subionospheric VLF perturbations, *J. Geophys. Res.*, *105*, 183–191, doi:10.1029/1999JA900329.
Tarcsai, G., P. Szemerdy, and L. Hegymegi (1988), Average electron density profiles in the plasmasphere between L = 1.4 and 3.2 deduced from whistlers, *J. Atmos. Terr. Phys.*, *50*(7), 607–611, doi:10.1016/0021-9169(88)90058-X.
Thomson, R. J., and R. L. Dowden (1977), Simultaneous ground and satellite reception of whistlers—1. Ducted whistlers, *J. Atmos. Terr. Phys.*, *39*, 869–877, doi:10.1016/0021-9169(77)90167-2.
Uman, M. A. (1984), *Lightning*, Dover, New York.
Uman, M. A. (2001), *The Lightning Discharge*, Dover, Mineola, N. Y.
Yip, W.-Y., U. S. Inan, and R. E. Orville (1991), On the spatial relationship between lightning discharges and propagation paths of perturbed subionospheric VLF/LF signals, *J. Geophys. Res.*, *96*, 249–258, doi:10.1029/90JA01997.

B. R. T. Cotts and M. A. Gołkowski, Department of Electrical Engineering, University of Colorado Denver, Denver, CO 80217, USA. (bcotts@exponent.com; mark.golkowski@ucdenver.edu)
R. C. Moore, Department of Electrical and Computer Engineering, University of Florida, 557 NEB, PO Box 116130, Gainesville, FL 32611, USA. (moore@ece.ufl.edu)